



# New half-sandwich ( $\eta^6$ -*p*-cymene)ruthenium(II) complexes with benzothiazole hydrazone Schiff base ligand: Synthesis, structural characterization and catalysis in transamidation of carboxamide with primary amines



Subbarayan Vijayapritha, Periasamy Viswanathamurthi\*

Department of Chemistry, Periyar University, Salem-636 011, India

## ARTICLE INFO

### Article history:

Received 2 April 2020

Revised 19 September 2020

Accepted 6 October 2020

Available online 7 October 2020

### Keywords:

Benzothiazole hydrazone Schiff bases

Ruthenium catalysts

Transamidation

Primary amines

Primary amides

## ABSTRACT

Few half-sandwich ( $\eta^6$ -*p*-cymene) ruthenium(II) complexes supported by benzothiazole hydrazone Schiff bases were synthesized. The new complexes possess the general formulae [Ru( $\eta^6$ -*p*-cymene)(L)Cl] (1-3) (L = salicyl((2-(benzothiazol-2-yl)hydrazone)methylphenol) (SAL-HBT), 2-((2-(benzothiazol-2-yl)hydrazone)methyl)-6 methoxyphenol) (VAN-HBT) or naphtyl-2-((2-(benzothiazol-2-yl)hydrazone)methyl phenol) (NAP-HBT). All compounds were fully studied by analytical, spectroscopic techniques (IR, NMR) and also by mass spectrometry. The solid state structure of the complex 3 reveals the coordination of *p*-cymene moieties with ruthenium(II) in a three-legged piano-stool geometry along with benzothiazole hydrazone Schiff base ligand in a monobasic bidentate fashion. The catalytic properties of the complexes were screened in transamidation of primary amide with amines after optimization with respect to solvent, substituents, time and catalyst loading. The results show that the complex 3 is the most efficient catalyst for the transamidation of carboxamides with amines.

© 2020 Elsevier B.V. All rights reserved.

## 1. Introduction

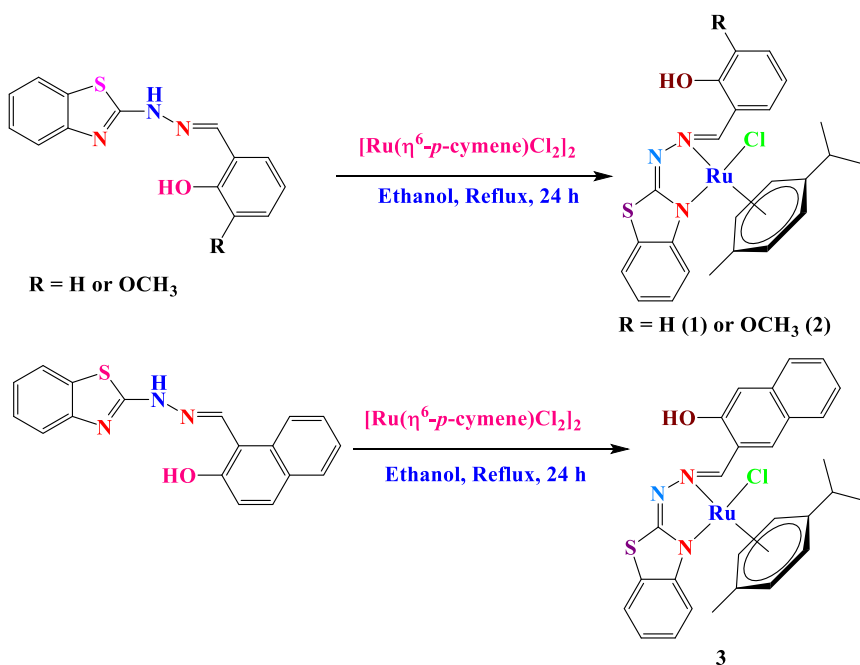
Amide functional groups present in numerous compounds ranging from biologically active natural products to pharmaceuticals [1]. Some examples of these include Lipitor (atorvastatin), fentanyl anaesthetic, metolachlor, capsaicin and nylon. They are also found within biological systems as the peptide bonds in proteins rendering them essential for life. As a result, several methods have been established for the synthesis of amides [2-6] including reactions of carboxylic acid derivatives (other than amides) with amines or ammonia [7], hydration of nitriles [5] and reaction of amines with aldehydes or alcohols [8] in addition to some recognized name reactions [9]. All of these methods possess their own merits along with certain shortcomings including utilization of stoichiometric amount of activating reagents, long reaction times, harsh reaction conditions, limited substrate scopes and formation of significant amount of chemical waste. In the search of cost-effective and more atom economical protocol, one of the methods employed to synthesis amide was transamidation, catalyzed by homogeneous transition metal catalysts. Stahl [10], Williams [11], Beller [12] and

other groups [13] reported elegant methods for transamidation by employing homogeneous transition metal catalytic systems. Among the homogeneous metal catalysts, Ru compounds emerged out to be the most promising candidate. In the past decade, many researchers utilized ruthenium metal catalysts for transmidation reaction including our own group [14]. Despite good results and advances were achieved in the previous reports, still it is interesting to synthesis new homogeneous catalysts with better catalytic activity.

In recent years, cyclometalated organometallic ruthenacycles flourish as an active class of catalysts. The aromatic  $\pi$ -ligand stabilizes and protects the metal centre from rapid oxidation [15]. These Ru(II) arene complexes display a three-legged piano stool structure creates the possibility of introducing different types of ligands into the octahedral metal centre [16] and also successfully utilized as better catalysts for several catalytic reactions such as C–H bond activation, hydrogenation reactions of unsaturated bonds of carbonyl, alkene and imines bonds, oxidative Heck reactions, oxidative C–C coupling and C–N coupling (amidation and hydroamination) [17-22]. The results of the above reactions show that varying the complex framework through modification of the arene ( $\eta^6$ R-arene) and the other auxiliary ligands is crucial for tuning chemical reactivity. In this context, many different supporting auxiliary ligands have

\* Corresponding author.

E-mail address: [viswanathamurthi@gmail.com](mailto:viswanathamurthi@gmail.com) (P. Viswanathamurthi).



**Scheme 1.** Schematic representation for the synthesis  $(\eta^6\text{-}p\text{-cymene})\text{Ru}(\text{II})$  complexes (1-3)

been used in combination with the Ru(II) arene scaffold to provide different reactivity profiles. The recent reports show that benzothiazole hydrazones attract considerable attention as versatile ligands since they possess both hard and soft donor atoms (e.g. NS or XNS, X = N, O, and S) in their skeleton [23].

Based on the above facts and continuation of our research on the synthesis, characterization and catalytic applications of transition metal based catalyst, we here in describe synthesis of three half-sandwich  $(\eta^6\text{-}p\text{-cymene})\text{Ru}(\text{II})$  complexes bearing benzothiazole hydrazone Schiff base ligand with different wingtip substituent in the benzene ring. The new complexes were characterized by analytical, spectroscopic techniques (IR, NMR), mass spectrometry and single crystal XRD. The synthesized complexes were used as catalysts in the transamidation of primary amide with amines. The effects of solvent, substituents, time and catalyst loading on the catalytic activity were also investigated.

## 2. Experimental

### 2.1. General strategy

Commonly available  $\text{RuCl}_3 \cdot 3\text{H}_2\text{O}$  was used as supplied from Sigma Aldrich. All chemicals and solvents were acquired from Merck or Aldrich. Thin-layer chromatography (Merck 1.05554 aluminum sheets precoated with silica gel 60 F254) was used for reaction observance and the spots were visualized with UV light at 254 nm or under iodine. Column chromatography refinement was done for the complexes using silica gel (200–400 mesh). Melting points were checked in open capillary tubes on a Technico micro heating table and are uncorrected. Infrared spectra of the compounds were obtained in the range of 4000–400  $\text{cm}^{-1}$  using Bruker alpha FT-IR spectrophotometer in ATR mode.  $^1\text{H}$  (400 MHz) and  $^{13}\text{C}$  (75.47 MHz) NMR spectra were recorded in  $\text{CDCl}_3$  at room temperature with a Bruker AV400 instrument using internal standard tetramethylsilane. Quadrupole time-of-flight Micro Analyzer (Shimadzu) mass spectrometry was used to measure electrospray ionization mass spectra (ESI) of compounds at SAIF, Panjab University, Chandigarh. Elemental analysis (C, H, N and S) were done on

a Vario EL III elemental analyzer. The ligands and metal precursor  $[\text{Ru}(\eta^6\text{-}p\text{-cymene})\text{Cl}_2]_2$  were prepared according to the previously published procedures [24,25].

### 2.2. Synthesis of ligands

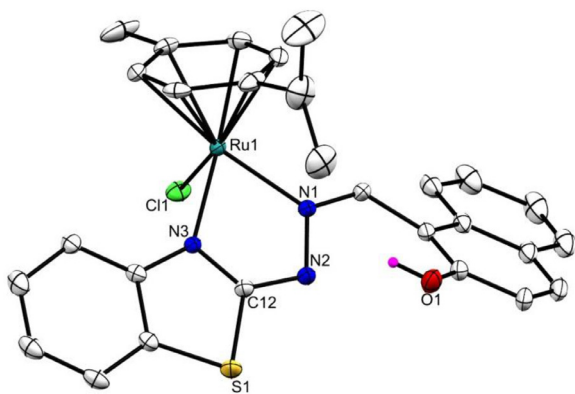
The following common procedure were used to synthesis all ligands. Typically, an ethanol (20 mL) solution of aldehyde (1 mmol) was added with 2-hydrazino benzothiazole (1 mmol) and the resulting mixture was stirred at room temperature for 5 h. The completion of the reaction was checked by Thin Layer Chromatography (TLC) and then the formed precipitate was filtered, washed using diethyl ether and air dried.

#### 2.2.1. Synthesis of (E)-2-((2-(benzo[d]thiazol-2-yl)hydrazinylidene)methyl)phenol (SAL-HBT)

The reaction of salicylaldehyde and 2-hydrazino benzothiazole was carried out for the synthesis of the ligand SAL-HBT. Yield: 88%; Color: White; M.p. 243 °C. Anal. Calcd for  $\text{C}_{14}\text{H}_{11}\text{ON}_3\text{S}$ : C, 62.43; H, 4.12; N, 15.60; S, 11.91%. Found: C, 62.56; H, 4.23; N, 15.79; S, 12.03%. IR (ATR,  $\text{cm}^{-1}$ ): 3352 (br,  $\nu_{\text{OH}}$ ); 3123 (w,  $\nu_{\text{NH}}$ ), 1573 + 1467 (s,  $\nu_{\text{C}=\text{N}} + \nu_{\text{C}-\text{N}}$ ), 747 (s,  $\nu_{\text{C}-\text{S}}$ ).  $^1\text{H}$  NMR (400 MHz,  $\text{CDCl}_3$ , ppm): 10.86 (s, 1H, OH), 8.38 (s, 1H,  $-\text{CH}=\text{N}$ ), 7.59–6.89 (m, 4H, Ar H), 4.25 (s, 1H, NH).  $^{13}\text{C}$  NMR (75.47 MHz,  $\text{CDCl}_3$ , ppm): 167.11 (S-C=N), 148.74 (C=N), 133.60 (Ar-C), 131.35 (Ar-C), 126.70 (Ar-C), 124.13 (Ar-C), 122.47 (Ar-C), 121.80 (Ar-C), 119.84 (Ar-C), 116.51 (Ar-C). ESI mass (m/z) calcd. for  $\text{C}_{14}\text{H}_{11}\text{N}_3\text{OS}$ , 269.32; Found, 270.41 [ $\text{M}+\text{H}]^+$ .

#### 2.2.2. Synthesis of (E)-2-((2-(benzo[d]thiazol-2-yl)hydrazinylidene)methyl)-6-methoxyphenol (VAN-HBT)

The reaction of o-vanillin and 2-hydrazino benzothiazole was carried out for the synthesis of the ligand VAN-HBT. Yield: 87%; Color: White; M.p. 210 °C. Anal. Calcd. for  $\text{C}_{15}\text{H}_{13}\text{O}_2\text{N}_3\text{S}$ : C, 60.18; H, 4.38; N, 14.04; S, 10.71%. Found: C, 60.27; H, 4.54; N, 14.16; S, 10.83%. IR (ATR,  $\text{cm}^{-1}$ ): 3574(br,  $\nu_{\text{OH}}$ ), 3145 (w,  $\nu_{\text{NH}}$ ), 1609 + 1469(s,  $\nu_{\text{C}=\text{N}} + \nu_{\text{C}-\text{N}}$ ), 773 (s,  $\nu_{\text{C}-\text{S}}$ ).  $^1\text{H}$  NMR (400 MHz,  $\text{CDCl}_3$ , ppm): 11.04

**Fig. 1.** Perspective view (50 % probability ellipsoids) of complex 3.**Table 1**  
Crystal data and structure refinement parameters for complex 3.

Parameter	Complex 3
CCDC Number	1981468
Empirical formula	C <sub>28</sub> H <sub>26</sub> ClN <sub>3</sub> ORuS
Formula weight	589.10
Temperature	296(2) K
Wavelength	0.71073 Å
Crystal system	Hexagonal
Space group	P-61
Unit cell dimensions	
a	17.5528(6) Å
b	17.5528(6) Å
c	16.2430(5) Å
α	90°
β	90°
γ	120°
Volume	4334.0(3) Å <sup>3</sup>
Z	6
Density (calculated)	1.354 Mg/m <sup>3</sup>
Absorption coefficient	0.731 mm <sup>-1</sup>
F(000)	1800
Crystal size	0.240×0.170×0.090 mm <sup>3</sup>
Theta range for data collection	1.340 to 29.002°.
Index ranges	-23<=h<=17, -23<=k<=23, -21<=l<=22
Reflections collected	27919
Independent reflections	7665 [R(int) = 0.0451]
Completeness to theta = 25.242°	99.8 %
Absortion correction	None
Refinement method	Full-matrix least-squares on F <sup>2</sup>
Data / restraints / parameters	7632 / 1 / 310
Goodness-of-fit on F <sup>2</sup>	1.144
Final R indices [I>2 sigma(I)]	R1 = 0.0487, wR2 = 0.1143
R indices (all data)	R1 = 0.0846, wR2 = 0.1400
Absolute structure parameter	0.002(16)
Extinction coefficient	n/a
Largest diff. peak and hole	0.844 and -0.605 e.Å <sup>-3</sup>

(s, 1H, OH), 8.39 (s, 1H, -CH=N), 7.51–6.84 (m, 7H, Ar H), 4.51 (s, 1H, NH), 3.93 (s, 3H, -OCH<sub>3</sub>). <sup>13</sup>C NMR (75.47 MHz, CDCl<sub>3</sub>, ppm): 167.12 (S-C=N), 153.34 (Ar-C), 151.01 (Ar-C), 148.42 (Ar-C), 146.78 (C=N), 126.37 (Ar-C), 125.11 (Ar-C), 124.12 (Ar-C), 122.05 (Ar-C), 120.83 (Ar-C), 119.46 (Ar-C), 117.50 (Ar-C), 56.35 (Ar-C). ESI mass (m/z) calcd. for C<sub>15</sub>H<sub>13</sub>N<sub>3</sub>O<sub>2</sub>S, 299.35; Found, 300.38 [M+H]<sup>+</sup>.

### 2.2.3. Synthesis of (E)-1-((2-(benzo[d]thiazol-2-yl)hydrazinylidene)methyl)naphthalen-2-ol (NAP-HBT)

The reaction of 2-hydroxy-1-naphthaldehyde and 2-hydrazino benzothiazole was carried out for the synthesis of the ligand NAP-HBT. Yield: 84%; Color: Yellow; M.p. 230 °C. Anal. Calcd for C<sub>18</sub>H<sub>13</sub>ON<sub>3</sub>S: C, 67.69; H, 4.10; N, 13.16; S, 10.04%. Found: C, 67.81;

**Table 2**  
Selected bond length [Å] and bond angle [°] for complex 3.

Bond length (Å)	Bond angle (°)
Ru(1)-N(3)	2.096(6)
Ru(1)-N(1)	2.105(6)
Ru(1)-Cl(1)	2.391(2)
Ru(1)-C(20)	2.239(8)
Ru(1)-C(21)	2.205(7)
Ru(1)-C(22)	2.171(9)
Ru(1)-C(23)	2.206(10)
Ru(1)-C(24)	2.143(9)
Ru(1)-C(25)	2.171(9)
N(3)-C(12)	1.300(10)
N(2)-C(12)	1.344(11)
N(3)-Ru(1)-N(1)	76.1(2)
N(3)-Ru(1)-Cl(1)	87.77(19)
N(1)-Ru(1)-Cl(1)	85.06(19)
N(2)-N(1)-Ru(1)	116.0(5)
N(3)-Ru(1)-C(24)	139.9(5)
N(1)-Ru(1)-C(24)	92.5(3)
N(3)-Ru(1)-C(22)	93.3(3)
N(1)-Ru(1)-C(22)	134.7(4)
C(24)-Ru(1)-C(22)	67.6(4)
C(12)-N(2)-N(1)	109.9(6)
C(13)-N(3)-Ru(1)	136.2(5)

H, 4.26; N, 13.29; S, 10.19%. IR (ATR, cm<sup>-1</sup>): 3630 (br, ν<sub>OH</sub>), 3066 (w, ν<sub>NH</sub>), 1582 + 1471 (s, ν<sub>C=N</sub> + ν<sub>C-S</sub>), 774 (s, ν<sub>C-S</sub>). <sup>1</sup>H NMR (400 MHz, CDCl<sub>3</sub>, ppm): 10.65 (s, 1H, OH), 8.10 (s, 1H, -CH=N), 7.96–7.22 (m, 10H, Ar H), 4.35 (s, 1H, NH). <sup>13</sup>C NMR (75.47 MHz, CDCl<sub>3</sub>, ppm): 168.46 (S-C=N), 156.27 (Ar-C), 148.44 (Ar-C), 142.49 (C=N), 132.63 (Ar-C), 129.28 (Ar-C), 128.52 (Ar-C), 128.15 (Ar-C), 126.03 (Ar-C), 125.85 (Ar-C), 123.95 (Ar-C), 122.13 (Ar-C), 121.12 (Ar-C), 108.61 (Ar-C), 105.68 (Ar-C). ESI mass (m/z) calcd. for C<sub>18</sub>H<sub>13</sub>N<sub>3</sub>OS, 319.38; Found, 320.39 [M+H]<sup>+</sup>.

### 2.3. Synthesis of new ruthenium complexes

All the complexes were synthesized by following general procedure. The precursor [Ru(*n*<sup>6</sup>-p-cymene)Cl<sub>2</sub>] (0.1 mmol) was treated with corresponding ligand (0.1 mmol) in ethanol (20 mL) for 24 h under reflux. During the course of the reaction, the color changed to orange. After completion of the reaction, a rotary evaporator was used to remove the solvent and the resulting crude product was dissolved in chloroform and then petroleum ether was added. The suspension was filtered and the orange solid was thoroughly washed with cold ethanol and diethyl ether.

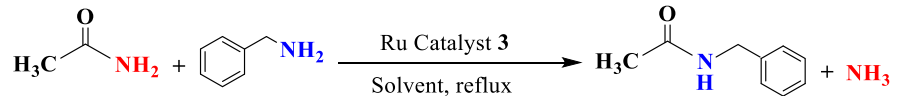
#### 2.3.1. Synthesis of [Ru(*n*<sup>6</sup>-p-cymene)(SAL-HBT)Cl] (**1**)

The ligand SAL-HBT was reacted with [Ru(*n*<sup>6</sup>-p-cymene)Cl<sub>2</sub>] for the synthesis of complex **1**. Yield: 74%; Color: Orange; M.p. 175 °C. Anal. Calcd. for C<sub>25</sub>H<sub>27</sub>ON<sub>3</sub>RuS: C, 54.19; H, 4.91; N, 7.58 S, 5.79%. Found: C, 54.35; H, 5.08; N, 7.69; S, 5.92 %. IR (ATR, cm<sup>-1</sup>): 3349 (br, ν<sub>OH</sub>), 1569 + 1461 (m, ν<sub>C=N</sub> + ν<sub>C-N</sub>), 756 (s, ν<sub>C-S</sub>). <sup>1</sup>H NMR (400 MHz, CDCl<sub>3</sub>, ppm): 11.02 (s, 1H, OH), 8.53 (s, 1H, -CH=N), 8.13–7.69 (m, 2H, Ar H), 7.51–6.97 (m, 6H, Ar H), 5.59 (d, J = 8 Hz, 1H, CH), 5.49 (d, J = 4 Hz, 1H, CH), 5.41 (d, J = 4 Hz, 1H, CH), 5.35 (d, J = 4 Hz, 1H, CH), 2.53 (s, 3H, CH<sub>3</sub>), 2.39 (sep, 1H, CH), 1.08 (d, J = 4 Hz, 3H, CH<sub>3</sub>), 0.92 (d, J = 4 Hz, 3H, CH<sub>3</sub>). <sup>13</sup>C NMR (75.47 MHz, CDCl<sub>3</sub>, ppm): 162.53 (C=N), 161.24 (S-C=N), 160.26 (Ar-C), 147.33 (Ar-C), 146.87 (Ar-C), 136.29 (Ar-C), 133.60 (Ar-C), 131.78 (Ar-C), 129.69 (Ar-C), 128.01 (Ar-C), 127.42 (Ar-C), 124.22 (Ar-C), 122.92 (Ar-C), 121.07 (Ar-C), 119.37 (Ar-C), 117.67 (Ar-C), 117.07 (Ar-C), 35.07 (CH), 22.87 (CH<sub>3</sub>), 22.19 (CH<sub>3</sub>), 21.57 (CH<sub>3</sub>). ESI mass (m/z) calcd. for C<sub>15</sub>H<sub>13</sub>N<sub>3</sub>O<sub>2</sub>S, 539.06; Found, 540.04 [M+H]<sup>+</sup>.

#### 2.3.2. Synthesis of [Ru(*n*<sup>6</sup>-p-cymene)(VAN-HBT)Cl] (**2**)

The ligand VAN-HBT was reacted with [Ru(*n*<sup>6</sup>-p-cymene)Cl<sub>2</sub>] for the synthesis of complex **2**. Yield: 76%; Color: Orange; M.p. 155 °C. Anal. Calcd. for C<sub>26</sub>H<sub>29</sub>O<sub>2</sub>N<sub>3</sub>RuS: C, 53.46; H, 5.00; N, 7.19; S, 5.49 %. Found: C, 53.62; H, 5.11; N, 7.33; S, 5.61 %. IR (ATR, cm<sup>-1</sup>): 3635 (br, ν<sub>OH</sub>); 1598 + 1460 (m, ν<sub>C=N</sub> + ν<sub>C-N</sub>); 760 (s, ν<sub>C-S</sub>). <sup>1</sup>H NMR (400 MHz, CDCl<sub>3</sub>, ppm): 11.73 (s, 1H, OH), 8.05 (s, 1H, -CH=N), 7.89–6.86 (m, 7H, Ar H), 5.48 (d, J = 8 Hz, 2H, CH), 5.35 (d, J = 4 Hz, 2H, CH), 3.96 (s, 3H, OCH<sub>3</sub>), 2.62 (s, 3H, CH<sub>3</sub>), 2.39 (sep, 1H, CH), 1.29 (d, J = 8 Hz, 3H, CH<sub>3</sub>), 1.13 (d, J = 4 Hz,

**Table 3**  
Evaluation of conditions for the model reaction using complex **3<sup>a</sup>**.

Entry	Catalyst (mol %)	Solvent	Temp (°C)	Time (h)	Yield (%) <sup>b</sup>		
						Ru Catalyst <b>3</b>	Solvent, reflux
1	0.1	1,4 dioxane	100	24	52		
2	0.25	1,4 dioxane	100	8	64		
<b>3</b>	<b>0.5</b>	<b>1,4 dioxane</b>	<b>100</b>	<b>8</b>	<b>93</b>		
4	1.0	1,4 dioxane	100	24	96		
5 <sup>c</sup>	0.5	1,4 dioxane	rt	24	n.r		
6	0.5	Acetonitrile	100	24	54		
7	0.5	DMF	110	24	9		
8	0.5	DMSO	110	24	18		
9	0.5	Chlorobenzene	110	24	29		
10	0.5	iPrOH	100	24	51		
11	0.5	1-Pentanol	110	24	n.r		
12	0.5	p-Xylene	110	24	73		
13	0.5	Ethanol	100	24	38		
14	0.5	Water	100	24	26		
15 <sup>d</sup>	0.5	-	100	24	n.r		
16 <sup>e</sup>	-	1,4 dioxane	100	24	n.r		

<sup>a</sup> Reaction conditions: Acetamide (5 mmol), benzyl amine (5 mmol), catalyst **3** in 5 mL of 1,4 dioxane.

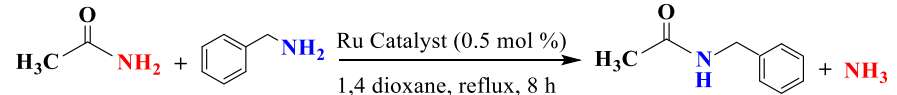
<sup>b</sup> Yields were calculated after isolation of the amide product through column chromatography using silica gel (200–400 mesh).

<sup>c</sup> Room temperature; n.r: no reaction.

<sup>d</sup> Without solvent.

<sup>e</sup> Without catalyst.

**Table 4**  
Selection of catalyst for transamidation reaction.<sup>a</sup>

Entry	Catalyst	Amount of catalyst (mol %)	Time (h)	Yield (%) <sup>b</sup>		
					Ru Catalyst (0.5 mol %)	1,4 dioxane, reflux, 8 h
1	1	0.5	8	78		
2	2	0.5	8	84		
<b>3</b>	<b>3</b>	<b>0.5</b>	<b>8</b>	<b>93</b>		

<sup>a</sup> Reaction conditions: Acetamide (5 mmol), benzyl amine (5 mmol), catalyst (0.5 mol %) in 5 mL of 1,4 dioxane, reflux at 100 °C.

<sup>b</sup> Yields were calculated after isolation of the amide product through column chromatography using silica gel (200–400 mesh).

3H, CH<sub>3</sub>). <sup>13</sup>C NMR (75.47 MHz, CDCl<sub>3</sub>, ppm): 162.51 (C=N), 161.12 (S-C=N), 151.70 (Ar-C), 147.70 (Ar-C), 147.21 (Ar-C), 146.52 (Ar-C), 136.92 (Ar-C), 131.95 (Ar-C), 129.69 (Ar-C), 127.34 (Ar-C), 125.41 (Ar-C), 124.05 (Ar-C), 123.56 (Ar-C), 122.98 (Ar-C), 119.72 (Ar-C), 117.60 (Ar-C), 114.41 (Ar-C), 56.35 (OCH<sub>3</sub>), 30.7 (CH), 23.19 (CH<sub>3</sub>), 22.57 (CH<sub>3</sub>), 21.58 (CH<sub>3</sub>). ESI mass (m/z) calcd. for C<sub>15</sub>H<sub>13</sub>N<sub>3</sub>O<sub>2</sub>S, 569.09; Found, 570.05 [M+H]<sup>+</sup>.

### 2.3.3. Synthesis of [Ru(*η*<sup>6</sup>-*p*-cymene)(NAP-HBT)Cl] (**3**)

The ligand NAP-HBT was reacted with [Ru(*η*<sup>6</sup>-*p*-cymene)Cl<sub>2</sub>]<sub>2</sub> for the synthesis of complex **3**. Yield: 71%; Color: Orange; M.p. 162 °C. Anal. Calcd for C<sub>29</sub>H<sub>29</sub>ON<sub>3</sub>RuSCl: C, 57.65; H, 4.84; N, 6.96; S, 5.31 %. Found: C, 57.77; H, 4.94; N, 7.09; S, 5.47 %. IR (ATR, cm<sup>-1</sup>): 3622 (br, ν<sub>OH</sub>), 1585 + 1480 (m, ν<sub>C=N</sub> + ν<sub>C-N</sub>), 780 (s, ν<sub>C-S</sub>). <sup>1</sup>H NMR (400 MHz, CDCl<sub>3</sub>, ppm): 10.95 (s, 1H, OH), 8.73 (s, 1H, –CH=N), 7.94–7.15 (m, 10H, Ar H), 5.72 (d, J = 4 Hz, 1H, CH), 5.68 (d, J = 8 Hz, 1H, CH), 5.48 (d, J = 4 Hz, 1H, CH), 5.34 (d, J = 8 Hz, 1H, CH), 2.69 (s, 3H, CH<sub>3</sub>), 2.41 (sep, 1H, CH), 1.02 (d, J = 4 Hz, 3H, CH<sub>3</sub>), 1.19 (d, J = 8 Hz, 3H, CH<sub>3</sub>). <sup>13</sup>C NMR (75.47 MHz, CDCl<sub>3</sub>, ppm): 164.47 (C=N), 163.56 (S-C=N), 156.94 (Ar-C), 148.24 (Ar-C), 145.77 (Ar-C), 137.71 (Ar-C), 134.91 (Ar-C), 131.32 (Ar-C),

128.85 (Ar-C), 8.68 (Ar-C), 127.86 (Ar-C), 127.70 (Ar-C), 126.88 (Ar-C), 124.75 (Ar-C), 123.88 (Ar-C), 120.14 (Ar-C), 116.67 (Ar-C), 30.78 (CH), 22.57 (CH<sub>3</sub>), 21.90 (CH<sub>3</sub>), 21.22 (CH<sub>3</sub>). ESI mass (m/z) calcd. for C<sub>15</sub>H<sub>13</sub>N<sub>3</sub>O<sub>2</sub>S, 589.12; Found, 590.06 [M+H]<sup>+</sup>. The slow evaporation of parent solution affords orange crystals suitable for single crystal XRD study.

### 2.4. Representative procedure for transamidation reaction

A mixture of amide (5 mmol), amine (5 mmol) and catalyst (0.5 mol %) in 1,4 dioxane (5 mL) was stirred in a sealed tube under nitrogen atmosphere at 100 °C for 8 h. Then the solvent was removed using rotavator and the resulting crude product was purified by column chromatography on silica gel (200–400 mesh) using eluents hexane and ethyl acetate [95:5, v/v] to afford corresponding amides as a white solid. The formation of products was confirmed by NMR spectroscopy. The reported isolated yields are an average of two runs.

**Table 5**  
Evaluations of substrate scope<sup>a,b</sup>.

<b>1 a</b> ( $R^1 = \text{methyl}$ ), 96%	<b>2 a</b> ( $R^1 = \text{methyl}$ ), 91%
<b>1 b</b> ( $R^1 = \text{tolyl}$ ), 92%	<b>2 b</b> ( $R^1 = \text{tolyl}$ ), 93%
<b>3 a</b> ( $R^1 = \text{methyl}$ ), 89%	<b>3 b</b> ( $R^1 = \text{tolyl}$ ), 85%
<b>4 a</b> ( $R^1 = \text{methyl}$ ), 72%	<b>5 a</b> ( $R^1 = \text{methyl}$ ), 74%
<b>4 b</b> ( $R^1 = \text{tolyl}$ ), 68%	<b>5 b</b> ( $R^1 = \text{tolyl}$ ), 69%
<b>6 a</b> ( $R^1 = \text{methyl}$ ), 67%	<b>7 a</b> ( $R^1 = \text{methyl}$ ), 65%
<b>6 b</b> ( $R^1 = \text{tolyl}$ ), 64%	<b>7 b</b> ( $R^1 = \text{tolyl}$ ), 62%
<b>8 a</b> ( $R^1 = \text{methyl}$ ), 70%	<b>9 a</b> ( $R^1 = \text{methyl}$ ), 77%
<b>8 b</b> ( $R^1 = \text{tolyl}$ ), 66%	<b>9 b</b> ( $R^1 = \text{tolyl}$ ), 73%
<b>10 a</b> ( $R^1 = \text{methyl}$ ), 78%	<b>11 a</b> ( $R^1 = \text{methyl}$ ), 81%
<b>10 b</b> ( $R^1 = \text{tolyl}$ ), 76%	<b>11 b</b> ( $R^1 = \text{tolyl}$ ), 80%
<b>12 a</b> ( $R^1 = \text{methyl}$ ), 83%	<b>13 a</b> ( $R^1 = \text{methyl}$ ), 93%
<b>12 b</b> ( $R^1 = \text{tolyl}$ ), 79%	<b>13 b</b> ( $R^1 = \text{tolyl}$ ), 91%
<b>14 a</b> ( $R^1 = \text{methyl}$ ), 95%	<b>15 a</b> ( $R^1 = \text{methyl}$ ), 94%
<b>14 b</b> ( $R^1 = \text{tolyl}$ ), 92%	<b>15 b</b> ( $R^1 = \text{tolyl}$ ), 90%

<sup>a</sup> Reaction conditions: Amide (5 mmol), amine (5 mmol), catalyst **3** (0.5 mol %) in 5 mL of 1,4 dioxane, reflux at 100°C for 8 h.

<sup>b</sup> Yields were calculated after isolation of the amide product through column chromatography using silica gel (200–400 mesh).

## 2.5. X-ray crystallographic study

Crystal of complex **3** was mounted on glass fiber, used for data collection. Crystal data were collected at 296 (2) K using a Gemini A Ultra Oxford Diffraction automatic diffractometer. Graphite monochromated Mo-K $\alpha$  radiation ( $\lambda = 0.71073 \text{ \AA}$ ) was used throughout. The absorption corrections were performed by the multi-scan method. Corrections were made for Lorentz and polarization effects. The structure was solved by direct methods using the program SHELXS. Refinement and all further calculations were carried out using SHELXL [26]. The H atoms were included in calculated positions and treated as riding atoms using the SHELXL default parameters. The non-hydrogen atoms were refined anisotropically using weighted full-matrix least squares on F<sup>2</sup>. Atomic scattering factors were incorporated into the computer programs.

## 3. Results and discussion

### 3.1. Synthesis and spectral characterization

The reaction of 2-hydrazino benzothiazole with salicylaldehyde, o-vanillin or 2-hydroxy-1-naphthaldehyde in ethanol gives the desired Schiff base ligands SAL-HBT, VAN-HBT or NAP-HBT in good yields. The reaction of ligands with [Ru( $\eta^6$ -p-cymene)Cl<sub>2</sub>]<sub>2</sub> in ethanol under reflux affords the new complexes

(**1–3**) (Scheme 1). All the complexes are non-hygroscopic solids, air-stable in solid state and solution at room temperature; soluble in common organic solvents such as acetone, benzene, chloroform, dichloromethane, dimethylsulfoxide, dimethylformamide, ethanol, methanol and insoluble in diethyl ether, hexane and petroleum ether. The complexes have been characterized by satisfactory elemental analyses, IR, <sup>1</sup>H, <sup>13</sup>C NMR and ESI-mass spectral studies. In addition, the solid-state structure of the complex **3** was confirmed by single crystal X-ray crystallography. The analytical data of the complexes are well matched with calculated values. Besides, the ESI-MS spectra of ligands and complexes (**1–3**) (Figs. S1–S6 in the supporting information) show that the molecular masses obtained for the compounds are complementary with theoretical molecular masses. Moreover, the fragmentation patterns also strongly support the formation of the intended compounds.

The information about the bonding between ligands and ruthenium metal in the synthesized complexes were predicted using IR spectra. The appearance of a broad signal at 3349–3635 cm<sup>−1</sup> in the ligands and complexes corresponding to  $\nu_{\text{OH}}$  indicates the non participation of phenolic –OH group in coordination with metal in complexes **1–3**. The spectra of ligands show a sharp signal at 3066–3145 cm<sup>−1</sup> due to  $\nu_{\text{NH}}$ . On complexation, the  $\nu_{\text{NH}}$  peak disappeared in the spectra of complexes (**1–3**) indicate –N=C=N tautomerism followed by deprotonation and coordination of benzothiazole ring nitrogen with metal. The presence of peak at 1573–1609 cm<sup>−1</sup>

in the spectra of ligands was assigned to imine group. However, in the spectra of complexes, the imine peak shifted to lower frequency and appeared at 1569–1598 cm<sup>-1</sup> reveal the participation of azomethine nitrogen in bonding with metal [27].

<sup>1</sup>H NMR spectroscopy is another tool to confirm the coordination of the ligands with the ruthenium metal. <sup>1</sup>H NMR analyses of all the compounds were done in deuterated solvent at room temperature (Figs. S7–S12 in the supporting information). The spectra of the free ligands show a singlet for OH protons at 11.04–10.65 ppm. The spectra of complexes also display peak in the region 11.73–10.95 ppm due to the non coordination of phenolic –OH group with metal in complexes **1–3**. The imine proton of ligands exhibits one singlet at around 8.53–8.05 ppm which is shifted to downfield in the spectra of complexes and appears at 8.39–8.10 ppm describes the coordination of imine nitrogen with ruthenium ion. The appearance of peak at 4.51–4.25 ppm in the ligands spectra was assigned to NH protons. The disappearance of NH proton signal in the complexes (**1–3**) indicates –N=C–NH tautomerism followed by deprotonation at benzothiazole ring nitrogen during the coordination with metal. The methoxy (OCH<sub>3</sub>) proton signal of ligand (VAN-HBT) and complex **2** was observed at 3.93 and 3.96 ppm respectively. All ruthenium complexes (**1–3**) display four doublets in the region 5.72–5.34 ppm and a singlet in the region 2.69–2.53 ppm corresponds to aromatic and methyl protons of the *p*-cymene. The methine proton of the *p*-cymene exhibits a septet in the range 2.41–2.39 ppm. The isopropyl group of the *p*-cymene shows two doublets at around 1.29–0.91 ppm. The diastrophic methyl protons of isopropyl group and chiral nature of the metal center may be the reason for the unusual splitting of the aromatic and isopropyl protons [28,29]. The above observations confirm the coordination of ligands with ruthenium ion and formation of desired complexes.

The <sup>13</sup>C NMR spectra of complexes **1–3** further support the formation of proposed complexes and the spectra show the expected signals in the appropriate regions (Figs. S13–S18 in the supporting information). The peak for imine carbon appears around 146.78–142.49 ppm for all the complexes (**1–3**). The aromatic carbons show signals in the region 160.26–114.41 ppm. The methoxy (OCH<sub>3</sub>) carbon signal was observed around 56.35 ppm for complex **2**. The methine (CH) carbon signal appears region at 35.07–30.78 ppm. The two isopropyl methyl carbons ((CH(CH<sub>3</sub>)<sub>2</sub>) of *p*-cymene exhibit signals at region 22.57–21.22 ppm and the methyl carbon (CH<sub>3</sub>) signal was observed at 23.19–22.57 ppm.

### 3.2. X-ray crystal structure of complex **3**

The solid-state structure of the complex **3** is shown in Fig. 1 and the summary of X-ray data and refinement parameters are displayed in Table 1. The selected bond lengths and angles for the complex **3** are shown in Table 2. The complex **3** was crystallized in “P-61” space group. The benzothiazole hydrazine ligands coordinated to Ru(II) ion as monobasic bidentate manner via imine nitrogen and benzothiazole ring nitrogen in all the complexes. The arene group of *p*-cymene is bonded to the metal ion in  $\eta^6$  fashion as centro symmetrically and a chloride ligand occupies the remaining position. Hence, the complexes exhibit a typical piano-stool conformation with pseudo octahedral geometry. The structural data of the complex are coincide with the formerly reported arene ruthenium(II) complexes [23].

Noteworthy in complex **3**, Ru(1)-N(1) and Ru(1)-N(3) bond lengths are 2.096(6) and 2.105(6) Å. The ruthenium-chloride bond length (2.239(8) Å) is higher than that of ruthenium nitrogen bond length. The ruthenium-carbon bond lengths 2.239(8), 2.205(7), 2.171(9), 2.206(10), 2.143(9) and 2.171(9) Å are comparable with earlier reported complexes [23]. The bond angle of N(3)-Ru(1)-N(1) in complex **3** is found to be 76.1(2) $^\circ$ . The N(3)-Ru(1)-Cl(1) and

N(1)-Ru(1)-Cl(1) bond angles (87.77 $^\circ$  and 85.06 $^\circ$ ) are close to that of an octahedral bond angle. This slight deviation from the octahedral bond angle is the evidence for attaining “piano stool” geometry. The bond lengths of N(2)-C(12) (1.344(11) Å) and C(12)-N(3) (1.300(10) Å) as well as absence of acidic NH proton confirm –N=C–NH tautomerism followed by deprotonation at benzothiazole ring nitrogen in solution during coordination with Ru metal ion.

### 3.3. Catalytic studies

Previous reports established that several ruthenium complexes were utilized as active catalysts in the synthesis of amides [30]. The reports revealed that the change in ligand design and substituent around metal center play major roles to increase the catalytic activity. Hence, the new complexes were subjected to screen their abilities to catalyze transamidation of carboxamides with amines. Generally, the transamidation of primary amides should be synthetically useful because it can provide a route to higher amides through expulsion of a molecule of ammonia. Thanks to its low boiling point, this can readily be removed from the reaction, providing secondary amides efficiently.

Initially, transamidation of primary amides was started using benchmark substrates acetamide and benzyl amine using complex **3** as catalyst. These substrates were selected in order to find optimization of various conditions such as presence of solvent, time and catalyst loading for the transamidation. The results of the preliminary reactions were shown in Table 3. In order to assess the crucial role of solvent, the solvent-dependent differences in the activities of catalysts were carried out on the model reaction using solvents such as *p*-xylene, chlorobenzene, acetonitrile, DMF, DMSO, 1-pentanol, *i*PrOH, ethanol, 1,4 dioxane and water. The ether like solvent 1,4 dioxane (Table 3, entry 3) was found to be better reaction media than protic solvents such as *i*PrOH, 1-pentanol, ethanol and water (Table 3, entries 10, 11, 13, 14). The polar aprotic solvents (DMF, DMSO) afford lower conversion (Table 3, entries 7, 8), whereas 1-pentanol prove completely futile (Table 3, entry 11). The non polar aromatic hydrocarbon such as *p*-xylene, chlorobenzene, have shown the yields of 29 % and 73 %. Acetonitrile could bring about conversion up to 54 %. Pleasantly, 1,4 dioxane was found to be the solvent of choice, giving 93 % yield in 8 h. To ensure the catalytic role of complex **3**, control experiment was performed in the absence of Ru(II) catalyst and solvent. As expected, no conversion takes place after a prolonged reaction time up to 24 h (Table 3, entries 15, 16).

We too explored the significance of catalyst loading and the results were depicted as Table 3. The catalyst loading of 0.5 mol % (Table 3, entry 3) leads to the maximum yield of 93 % for catalyst **3** with in 8 h. However, decrease the catalyst amount in transamidation reaction result corresponding product in lower yield even after 24 h (Table 3, entry 1, 2). Higher catalyst loading (1 mol %) leads to slightly higher yield after 24 h (Table 3, entry 1, 2). From the results, 0.5 mol % was considered to be the choice of catalyst loading. Additionally, catalyst **3** was found to be the best catalyst for transamidation reaction to obtain excellent yield (Table 4, entry 3). Other catalysts such as **1** and **2** show lower activity than the catalyst **3** (Table 4, entry 1, 2). The overall catalytic activity of the complexes is in the order **3** > **2** > **1**. The higher catalytic activity of catalyst **3** is due to the presence of bulky planar naphthalene ring system in the ligand.

In order to know the general applicability and versatility of the synthesized catalyst, we have conducted a series of catalytic transamidation reactions using the complex **3** as catalyst under optimized conditions. Various substituted primary amines were reacted with primary amide such as acetamide or 4-methyl benzamide under optimized conditions and the % yields were tabulated in Table 5. The aromatic amine like benzyl amine, ani-

line, 2-naphthyl amine showed the very high yields. (1a-b, 2a-b, 3a-b). Electron with drawing groups (4a-b, 5a-b & 6a-b) as well as electron donating groups (7a-b, 8a-b) on both ortho, meta and para positions were well tolerated by the catalytic system and showed moderate yields under optimized conditions. Further, heteroatom containing amines such as 2-picoly amine was also perfectly adopted and underwent transamidation with high yield (13a-b) compared to aniline derivatives which may due to the presence of basic nitrogen atom in aromatic ring. Next, the steric effect was studied and it was found that various substituted aniline like 2,6 dimethyl aniline (9a-b), 2,6-diethyl aniline (10a-b), 2,4,6-trimethyl aniline (11a-b), 2,6 diisopropyl aniline (12a-b) provided moderate to good yields. The nature of substituents and their positions have shown influence over the reaction. In general, the *p*-nitro aniline, as expected due to its decreased nucleophilicity provides moderate yields (5a-b). The less nucleophilicity in *m*-chloro aniline significantly reduced the yield (6a-b). This may be due to the delocalization of nitrogen lone pair of electrons on the aromatic ring which is apparent according to the literature [11a]. The presence of aliphatic groups like cyclohexylamine and tertiary butyl amine enhanced the yields (14a-b, 15a-b).

#### 4. Conclusions

Synthesis, structural characterization and catalytic activity of half-sandwich ( $\eta^6$ -*p*-cymene) Ruthenium(II) complexes were presented in this work. The benzothiazole hydrazone Schiff base ligands coordinated with Ru(II) ion as monobasic bidentate N-N fashion. The pseudo-octahedral "piano-stool" geometry compensated by *p*-cymene ring ( $\eta^6$ ), one Cl and monobasic bidentate (N-N) benzothiazole hydrazone Schiff base ligands have been revealed by single crystal X-ray diffraction study (Complex **3**). Moreover, the synthesized complexes were screened as catalyst in transamidation of primary amides. The catalytic transamidation reactions give good to excellent yields which exhibit the stability of the complexes towards the atmospheric conditions. By comparing the catalytic activity of complexes [**1-3**], the complex **3** has been confirmed as an effectual and suitable catalyst under milder reaction condition. The designed protocol is highly suitable in terms of synthesis because the starting material used has been readily available no harmful reactive reagents or without forming wasteful byproducts.

#### Declaration of Competing Interest

The authors declare that they have no known competing financial interests or personal relationships that could have appeared to influence the work reported in this paper.

#### CRediT authorship contribution statement

**Subbarayan Vijayapritha:** Conceptualization, Investigation, Writing - original draft. **Periasamy Viswanathamurthi:** Validation, Methodology, Formal analysis, Writing - review & editing, Visualization, Supervision, Project administration.

#### Acknowledgements

We thank Department of Chemistry, Gandhigram Rural Institute-Deemed University, Gandhigram (NMR spectra) and SAIF, Gauhati University, Guwahati (single crystal X-Ray) for their help in characterization studies.

#### Supplementary materials

Supplementary material associated with this article can be found, in the online version, at doi:10.1016/j.jorgchem.2020.121555.

#### References

- [1] W. Ding, S. Mai, Q. Song, Beilstein J. Org. Chem. 11 (2015) 2158–2165.
- [2] J. Kim, H.J. Kim, S. Chang, Eur. J. Org. Chem. (2013) 3201–3213.
- [3] C.L. Allen, J.M. Williams, Chem. Soc. Rev. 40 (2011) 3405–3415.
- [4] (a) F. El-Faham, Albericio, Chem. Rev. 111 (2011) 6557–6602; (b) R.M. Lanigan, P. Starkov, T.D. Sheppard, J. Org. Chem. 78 (2013) 4512–4523.
- [5] R. Garcia-Alvarez, P. Crochet, V. Cadiero, Green Chem. 15 (2013) 46–66.
- [6] (a) J.F. Soule, H. Miyamura, S. Kobayashi, J. Am. Chem. Soc. 133 (2011) 18550–18553; (b) K. Yamaguchi, H. Kobayashi, T. Oishi, N. Mizuno, Angew. Chem. Int. Ed. 51 (2012) 544–547; (c) A. Sakakura, T. Ohkubo, R. Yamashita, M. Akaura, K. Ishihara, Org. Lett. 13 (2011) 892–895; (d) A. Sakakura, R. Yamashita, T. Ohkubo, M. Akaura, K. Ishihara, Aust. J. Chem. 64 (2011) 1458–1465; (e) S.C. Ghosh, J.S.Y. Ngiam, A.M. Seayad, D.H. Tuan, C.L. Chai, A. Chen, J. Org. Chem. 77 (2012) 8007–8015.
- [7] (a) C.A.G.N. Montalbetti, V. Falque, Tetrahedron 61 (2005) 10827–10852; (b) E. Valeur, M. Bradley, Chem. Soc. Rev. 38 (2009) 606–631.
- [8] (a) H. Nambu, K. Hata, M. Matsugi, Y. Kita, Chem. Eur. J. 11 (2005) 719–727; (b) C. Gunanathan, Y. Ben-David, D. Milstein, Science 317 (2007) 790–792; (c) K. Ekoue-Kovi, C. Wolf, Chem. Eur. J. 14 (2008) 6302–6315; (d) J.B. Gaultierotti, X. Schumacher, P. Fontaine, G. Masson, Q. Wang, J. Zhu, Chem. Eur. J. 18 (2012) 14812–14819; (e) K. Xu, Y. Hu, S. Zhang, Z. Zha, Z. Wang, Chem. Eur. J. 18 (2012) 9793–9797.
- [9] L. Kurti, B. Czako, Strategic Applications of Named Reactions in Organic Synthesis, Elsevier Academic Press, Amsterdam, The Netherlands, 2005.
- [10] (a) S.E. Eldred, D.A. Stone, S.H. Gellman, S.S. Stahl, J. Am. Chem. Soc. 125 (2003) 3422–3423; (b) N.A. Stephenson, J. Zhu, S.H. Gellman, S.S. Stahl, J. Am. Chem. Soc. 131 (2009) 10003–10008.
- [11] (a) C.L. Allen, B.N. Atkinson, J.M. Williams, Angew. Chem. Int. Ed. 51 (2012) 1383–1386; (b) B.N. Atkinson, A.R. Chhatwal, H.V. Lomax, J.W. Walton, J.M. Williams, Chem. Commun. 48 (2012) 11626–11628.
- [12] M. Zhang, S. Imm, S. Bahn, L. Neubert, H. Neumann, M. Beller, Angew. Chem. Int. Ed. 51 (2012) 3905–3909.
- [13] (a) J.E. Dander, E.L. Baker, N.K. Garg, Chem. Sci. 8 (2017) 6433–6438; (b) L. Bercera-Figueroa, A. Ojeda-Porras, D. Gamba-Sanchez, J. Org. Chem. 79 (2014) 4544–4552; (c) G. Meng, P. Lei, M. Szostak, Org. Lett. 19 (2017) 2158–2161; (d) M. Tamura, T. Tonomura, K. Shimizu, A. Satsuma, Green Chem. 14 (2012) 717–724.
- [14] (a) M. Nirmala, G. Prakash, P. Viswanathamurthi, J. Mol. Catal. A: Chem. 403 (2015) 15–26; (b) M. Nirmala, R. Manikandan, G. Prakash, P. Viswanathamurthi, App. Organometal. Chem. 28 (2014) 18–26; (c) R. Manikandan, P. Anitha, G. Prakash, P. Vijayan, P. Viswanathamurthi, R.J. Butcher, J.G. Malecki, J. Mol. Catal. A: Chem. 398 (2015) 312–324; (d) M. Nirmala, P. Viswanathamurthi, J. Chem. Sci. 128 (2016) 9–21; (e) M. Nirmala, P. Viswanathamurthi, J. Chem. Sci. 128 (2016) 1725–1735; (f) S. Selvamurugan, R. Ramachandran, G. Prakash, P. Viswanathamurthi, J.G. Malecki, A. Endo, J. Organometal. Chem. 803 (2016) 119–127; (g) M. Nirmala, G. Saranya, P. Viswanathamurthi, Inorg. Chim. Acta 442 (2016) 134–144; (h) S. Selvamurugan, R. Ramachandran, G. Prakash, M. Nirmala, P. Viswanathamurthi, S. Fujiwara, A. Endo, Inorg. Chim. Acta 454 (2017) 46–53.
- [15] Y. Fu, M.J. Romero, A. Habtemariam, M.E. Snowden, L. Song, G.J. Clarkson, B. Qamar, A.M. Pizarro, P.R. Unwin, P.J. Sadler, Chem. Sci. 3 (2012) 2485–2494.
- [16] P. Kumar, R.K. Gupta, D.S. Pandey, Chem. Soc. Rev. 43 (2014) 707–733.
- [17] (a) M. Hiranoa, S. Komiya, Coord. Chem. Rev. 314 (2016) 182–200; (b) P.B. Arockiam, C. Bruneau, P.H. Dixneuf, Chem. Rev. 112 (2012) 5879–5918; (c) B.M. Trost, F.D. Toste, A.B. Pinkerton, Chem. Rev. 101 (2001) 2067–2096; (d) V. Ritleng, C. Sirlin, M. Pfeffer, Chem. Rev. 102 (2002) 1731–1770; (e) Y. Na, S. Park, S.B. Han, H. Han, S. Ko, S. Chang, J. Am. Chem. Soc. 126 (2004) 250–258; (f) R. Manikandan, P. Madasamy, M. Jeganmohan, ACS Catal. 6 (2016) 230–234; (g) J. Hubrich, T. Himmler, L. Rodefeld, L. Ackermann, ACS Catal. 5 (2015) 4089–4093; (h) M. Zhang, Y. Zhang, X. Jie, H. Zhao, G. Li, W. Su, Org. Chem. Front. 1 (2014) 843–895; (i) A. Biafora, F.W. Patureau, Synlett 25 (2014) 2525–2530; (j) K. Shin, H. Kim, S. Chang, Acc. Chem. Res. 48 (2015) 1040–1052; (k) S. Raoufmoghaddam, Org. Biomol. Chem. 12 (2014) 7179–7193; (l) L. Ackermann, Org. Lett. 7 (2005) 3123–3125; (m) P.B. Arockiam, C. Fischmeister, C. Bruneau, P.H. Dixneuf, Angew. Chem. Int. Ed. 49 (2010) 6629–6632; (n) L. Ackermann, S. Fenner, Org. Lett. 13 (2011) 6548–6551.
- [18] (a) D. Tyagi, C. Binnani, R.K. Rai, A.D. Dwivedi, K. Gupta, P.Z. Li, Y. Zhao, S.K. Singh, Inorg. Chem. 55 (2016) 6332–6343; (b) K.Y. Ghebreyessus, J.H. Nelson, J. Organomet. Chem. 669 (2003) 48–56.
- [19] P. Nareddy, F. Jordan, M. Szostak, ACS Catal. 7 (2017) 5721–5745.
- [20] (a) X. Yun, J. Zhu, Y. Jin, W. Deng, Z. Yao, Inorg. Chem. 59 (2020) 7841–7851; (b) M.M. Sheeba, M. Muthu Tamizh, L.J. Farrugia, A. Endo, R. Karvembu, Organometallics 33 (2014) 540–550.
- [21] (a) S. Bauri, S.N.R. Donthireddy, P.M. Illam, A. Rit, Inorg. Chem. 57 (2018) 14582–14593; (b) S. Saranya, R. Ramesh, D. Semeril, Organometallics 39 (2020) 3194–3201.

- [22] A.M. Pizarro, M. Melchart, A. Habtemariam, L. Salassa, F.P.A. Fabbiani, S. Parsons, P.J. Sadler, Inorg. Chem. 49 (2010) 3310–3319.
- [23] (a) L. Dkhar, W. Kaminsky, K.M. Poluri, M.R. Kollipara, J. Organometal. Chem. 891 (2019) 54–63; (b) L. Dkhar, V. Banothu, W. Kaminsky, M.R. Kollipara, J. Organometal. Chem. 914 (2020) 121225.
- [24] M. Ghorbanloo, R. Bikas, G. Małecki, Inorg. Chim. Acta 445 (2016) 8–16.
- [25] M.A. Bennett, T.N. Huang, T.W. Matheson, A.K. Smith, Inorg. Synth. 21 (2007) 74–78.
- [26] G.M. Sheldrick, Acta Crystallogr. Sect. A 64 (2008) 112–122.
- [27] S. Vijayapritha, K. Murugan, P. Viswanathamurthi, P. Vijayan, C. Kalaiarasi, Inorg. Chim. Acta 512 (2020) 119887–119897.
- [28] M. Nirmala, M. Adinarayana, K. Ramesh, M. Maruthupandi, M. Vaddamanu, G. Raju, G. Prabusankar, New J. Chem. 42 (2018) 15221–15230.
- [29] S. Adhikari, O. Hussain, R.M. Phillips, W. Kaminsky, M.R. Kollipara, Appl. Organometal. Chem. 32 (2018) e4362–e4375.
- [30] (a) M.H.G. Prechtl, K. Wobser, N. Theyssen, Y.B. David, D. Milstein, W. Leitner, Catal. Sci. Technol. 2 (2012) 2039–2042; (b) R.M. Lanigan, T.D. Sheppard, Eur. J. Org. Chem. 33 (2013) 7453–7465.